Progress In Electromagnetics Research, Vol. 113, 127–141, 2011

HYBRID TANGENTIAL EQUIVALENCE PRINCIPLE ALGORITHM WITH MLFMA FOR ANALYSIS OF ARRAY STRUCTURES

H. Shao, J. Hu, Z. Nie, G. Han, and S. He

School of Electronic Engineering
University of Electronic Science and Technology of China
Chengdu, Sichuan 611731, China

Abstract—In this paper, a novel technique is proposed to solve the electromagnetic scattering by large finite arrays by combining the tangential equivalence principle algorithm (T-EPA) with multilevel fast multipole algorithm (MLFMA). The equivalence principle algorithm (EPA) is a kind of domain decomposition scheme for the electromagnetic scattering and radiation problems based on integral equation (IE). For the array with same elements, only one scattering matrix needs to be constructed and stored. T-EPA has better accuracy than the original EPA. But the calculation for the impedance matrix in T-EPA is still time consuming. MLFMA is proposed to speed up the matrix-vector multiplication in T-EPA. Numerical results are shown to demonstrate the accuracy and efficiency of the proposed technique.

1. INTRODUCTION

In recent years, research on the radar cross section (RCS) of array antennas has received much attention because the scattering from the array mounted on a low-observable platform may give significant contribution to the overall RCS [1–4]. To accurately model the currents on the array element and the mutual coupling among the elements, a three dimensional (3D) full-wave analysis is necessary. Plenty of numerical techniques have been proposed to address the problems of large arrays such as the method of moments (MoM) [5, 6], finite element method (FEM) [7–10] and finite-difference time-domain method (FDTD) [11]. As a popular integral equation method (IEM), the MoM has been widely used for numerical analysis of

Received 22 December 2010, Accepted 24 January 2011, Scheduled 28 January 2011
Corresponding author: Jun Hu (hujun@uestc.edu.cn).

electromagnetic problems. By comparison with experiment results for various antenna configurations, the high accuracy of the MoM has been verified. However, the memory requirement and CPU time in MoM are $O(N^2)$ for iterative solvers, where N denotes the number of unknowns. In last decades, many fast algorithms, such as multilevel fast multipole algorithm (MLFMA) [12–19], adaptive integral method (AIM) [20, 21], integral equation fast fourier transform (IE-FFT) [22, 23], have been proposed to improve the numerical efficiency of the IE significantly. But these fast methods are not most suitable for problems of finite arrays.

The equivalence principle algorithm (EPA), based on the domain decomposition method (DDM) and surface equivalence principle, has been developed to solve multi-scale problems and array structures with same elements [24–27]. This algorithm utilizes virtual equivalence surfaces to enclose objects and transfers original unknowns of the objects onto the new unknowns of the equivalence surfaces. The surface integral equation is used on virtual equivalence surfaces. If the objects consist of complex perfect electric conductor (PEC) structures or high permittivity dielectrics, the unknowns of the equivalence surfaces will be much less than the unknowns on the objects. Therefore, the EPA can reduce the number of unknowns significantly. For array with the same elements, only one scattering matrix needs to be solved and stored, which can reduce the memory requirement significantly. The other benefit of EPA method is that it can improve the conditioning of the impedance matrix. A similar DDM method named generalized transition matrix is discussed in [28].

In this paper, the EPA is applied to solve the electromagnetic scattering of periodic array and non-periodic array. But when the equivalence surfaces are close to the objects, the original EPA leads to a loss of accuracy. To improve the accuracy of the traditional EPA, tangential EPA (T-EPA) has been developed [29–31]. To further reduce the memory requirement and CPU time, MLFMA is applied in T-EPA to speed up the computations of interactions among equivalence surfaces. Numerical results are shown to demonstrate the accuracy and efficiency of the T-EPA hybrid with MLFMA for solving the array structures.

2. EQUIVALENCE PRINCIPLE ALGORITHM

The electromagnetic scattering of a number of disjoint objects P_l, $(l = 1, \ldots, N)$ in free space is investigated, where N is the number of objects. In EPA, those objects are divided into groups. Each group is enclosed by an virtual equivalence surface ES_l, $(l = 1, \ldots, K)$, where

K is the number of equivalence surfaces. All of the equivalence surfaces are disjoint. The EPA method is mainly based on two procedures: the scattering of objects via an equivalence surface and the interaction among the equivalence surfaces. The first procedure is described by the scattering operators $\mathbf{S}_{ll}$, (l=1,...,K), which contain the information of the inside objects. The scattering operators $\mathbf{S}_{ll}$ are defined to compute the scattering currents on the equivalence surfaces. For the PEC objects, the $\mathbf{S}_{ll}$ can be written as [24]

$$\mathbf{S}_{ll} = \begin{bmatrix} \hat{n} \times K_{lp} \\ \eta_0 L_{lp} \times \hat{n} \end{bmatrix} \cdot \begin{bmatrix} \eta_0 L_{pp} \end{bmatrix}^{-1} \cdot \begin{bmatrix} \eta_0 L_{pl} & -K_{pl} \end{bmatrix} \tag{1}$$

Here, the subscript l and p represent the equivalence surface and the PEC object inside the equivalence surface respectively. The L and K are the surface integral operators defined as

$$L\left(\mathbf{X}\left(\mathbf{r}'\right)\right) = -jk\eta_0 \int_S \left[\mathbf{X}\left(\mathbf{r}'\right) + \frac{1}{k^2}\nabla\nabla' \cdot \mathbf{X}\left(\mathbf{r}'\right)\right] G_0 ds' \tag{2}$$

$$K\left(\mathbf{X}\left(\mathbf{r}'\right)\right) = \int_S \nabla G_0 \times \mathbf{X}\left(\mathbf{r}'\right) ds' \tag{3}$$

Here, $\mathbf{X}$ is $\mathbf{J}$ or $\mathbf{M}$, G_0 is the Green's function in free space. η_0 is the wave impedance in free space. Using the scattering operators $\mathbf{S}_{ll}$, the unknowns of the objects are transferred onto the unknowns of the equivalence surfaces. Then the new unknowns are the equivalence electric and magnetic currents $\mathbf{J}_l^s = \hat{n}_l \times \mathbf{H}_l^s$ and $\mathbf{M}_l^s = -\hat{n}_l \times \mathbf{E}_l^s$ on ES_l, $(l = 1, \ldots, K)$, where $\hat{n}_l$ denotes the unit outer normal vector on the ES_l. The $\mathbf{E}_l^s$ and $\mathbf{H}_l^s$ denote the electric and magnetic fields on the ES_l respectively. The interactions between two equivalence surfaces ES_l and ES_k, $(k \neq l)$ are described by the translation operators $\mathbf{T}_{lk}$, $(k \neq l)$ as [24]

$$\mathbf{T}_{lk} = \begin{bmatrix} \hat{n} \times K_{lk} & \frac{1}{\eta_0}\hat{n} \times L_{lk} \\ -\eta_0 \times L_{lk} & \hat{n} \times K_{lk} \end{bmatrix} \tag{4}$$

Figure 1 shows an example of the interaction between two PEC objects using EPA method.

Finally, the discretized form of EPA equation on equivalence surfaces can be represented as:

$$\begin{bmatrix} \mathbf{I} & -\mathbf{S}_{11}\mathbf{T}_{12} & \cdots & -\mathbf{S}_{11}\mathbf{T}_{1K} \\ -\mathbf{S}_{22}\mathbf{T}_{21} & \mathbf{I} & \cdots & -\mathbf{S}_{22}\mathbf{T}_{2K} \\ \vdots & \vdots & \ddots & \vdots \\ -\mathbf{S}_{KK}\mathbf{T}_{K1} & \cdots & \cdots & \mathbf{I} \end{bmatrix} \cdot \begin{bmatrix} \mathbf{V}_1^s \\ \mathbf{V}_2^s \\ \vdots \\ \mathbf{V}_K^s \end{bmatrix} = \begin{bmatrix} \mathbf{S}_{11}\mathbf{V}_1^i \\ \mathbf{S}_{22}\mathbf{V}_2^i \\ \vdots \\ \mathbf{S}_{KK}\mathbf{V}_K^i \end{bmatrix} \tag{5}$$

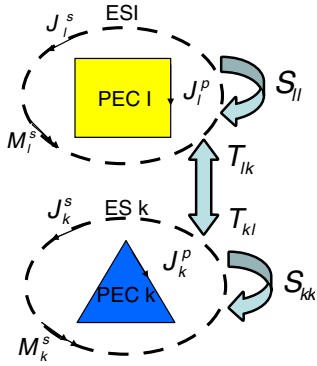

Figure 1. The interaction between two PEC objects using EPA method.

where $\mathbf{I}$ is the identity operator,

$$\mathbf{V}_l^{i/s} = \begin{bmatrix} \mathbf{J}_l^{i/s} \\ \mathbf{M}_l^{i/s} \end{bmatrix} \tag{6}$$

are the incident or scattering equivalence currents on the ES_l, $(l = 1, \ldots, K)$. After solving the equivalence surface currents $\mathbf{J}_l^s$ and $\mathbf{M}_l^s$, the scattering fields can be derived outside the equivalence surfaces.

3. TANGENTIAL EQUIVALENCE PRINCIPLE ALGORITHM

In traditional EPA, the equivalence surface currents $\mathbf{J}$ and $\mathbf{M}$ are the rotated tangential projections of the fields onto the surface. Equation (7) is used to solve the $\mathbf{J}$ and $\mathbf{M}$.

$$\begin{bmatrix} \mathbf{I} & 0 \\ 0 & \mathbf{I} \end{bmatrix} \cdot \begin{bmatrix} \mathbf{J} \\ \mathbf{M} \end{bmatrix} = \begin{bmatrix} \hat{n} \times \mathbf{H} \\ -\hat{n} \times \mathbf{E} \end{bmatrix} \tag{7}$$

Here, $\mathbf{E}$ and $\mathbf{H}$ denote the known fields. Curvilinear Rao-Wilton-Glisson (CRWG) basis functions [32, 33] are used to expand the currents $\mathbf{J}$ and $\mathbf{M}$. The equation is tested with Galerkin's scheme. Numerical experiments show that the computed fields lead to a lose of accuracy if the equivalence surfaces close to the inside objects. T-EPA has been proposed to improve the accuracy of the original EPA. The idea is to utilize tangential integrodifferential operators in projecting the fields onto the surface currents. The $\mathbf{J}$ and $\mathbf{M}$ are represented in

terms of basis functions. The T-EPA equation can be written as [29]

$$\begin{bmatrix} \eta_0 L & -K \\ K & \frac{1}{\eta_0} L \end{bmatrix} \cdot \begin{bmatrix} \mathbf{J} \\ \mathbf{M} \end{bmatrix} = \begin{bmatrix} \mathbf{E} \\ \mathbf{H} \end{bmatrix} \tag{8}$$

To do this, the scattering operator $\mathbf{S}_{ll}$ and translation operator $\mathbf{T}_{lk}$ have to be modified as

$$\mathbf{S}_{ll}^{t} = \begin{bmatrix} \eta_0 L_{lp} \\ K_{lp} \end{bmatrix} \cdot \begin{bmatrix} \eta_0 L_{pp} \end{bmatrix}^{-1} \cdot \begin{bmatrix} \eta_0 L_{pl} & -K_{pl} \end{bmatrix} \tag{9}$$

and

$$\mathbf{T}_{lk}^{t} = \begin{bmatrix} \eta_0 L_{lk} & -K_{lk} \\ K_{lk} & \frac{1}{\eta_0} L_{lk} \end{bmatrix} \tag{10}$$

where the superscript t denotes tangential projections. Another method using high-order field point sampling scheme is applied to improve the accuracy of the original EPA [27].

4. ACCELERATIONS OF T-EPA USING MLFMA

In [30, 31], T-EPA has been used to analysis of array dielectric spheres and metamaterial structures. Although T-EPA can reduce the final number of unknowns, it is still very time consuming for large arrays. As well known, MLFMA is used to accelerate the matrix-vector multiplication with the complexity of $O(N \log N)$. In this paper, MLFMA [13] is applied in the T-EPA to accelerate the translation procedure in which all the equivalence surface currents interact with each other. Equation (5) is rewritten as

$$\begin{bmatrix} \mathbf{J}^s \\ \mathbf{M}^s \end{bmatrix} - \begin{bmatrix} \mathbf{S} \end{bmatrix} \cdot \begin{bmatrix} \mathbf{T} \end{bmatrix} \cdot \begin{bmatrix} \mathbf{J}^s \\ \mathbf{M}^s \end{bmatrix} = \begin{bmatrix} \mathbf{S} \end{bmatrix} \cdot \begin{bmatrix} \mathbf{J}^i \\ \mathbf{M}^i \end{bmatrix} \tag{11}$$

Because the equivalence surface currents do not radiate to the self equivalence surface, the self interaction of each equivalence surface must be excluded. Then the translation matrix $\mathbf{T}$ has zeros on the diagonal blocks. But MLFMA is usually used to compute a fully dense matrix-vector multiplication. In this letter, the self interaction of each equivalence surface is subtracted after matrix-vector multiplication.

For L operators in the translation matrix $\mathbf{T}$, the radiation and receiving patterns have the same form as

$$\mathbf{V}_{smi}^{E}\left(\hat{k}\right) = \int_S \left[\bar{\mathbf{I}} - \hat{k}\hat{k}\right] \cdot e^{i\mathbf{k}\cdot(\mathbf{r}_m - \mathbf{r}_i)} \cdot \mathbf{f}_i(\mathbf{r}_m - \mathbf{r}_i) ds \tag{12}$$

where $\mathbf{r}_m$ is the center position of group m, $\mathbf{r}_i$ is the location of the sampling point. The radiation patterns of K operators are

$$\mathbf{V}_{smi}^{M}\left(\hat{k}\right) = \int_S \hat{k} \times e^{i\mathbf{k}\cdot(\mathbf{r}_m - \mathbf{r}_i)} \cdot \mathbf{f}_i(\mathbf{r}_m - \mathbf{r}_i) ds \tag{13}$$

The receiving pattern of K operators are the same as L operators. The symmetry in radiation and receiving patterns is also applied to further reduce the total memory requirement [36].

It is necessary to point out that there are some limitations of the present EPA method: (1) The distance between the equivalence surface and the object should be chosen carefully. The distance should be larger than one tenth of wavelength in order to maintain a good precision, and not be too far in order to reduce the number of unknowns on the equivalence surface. (2) For calculating the scattering matrix **S** in the EPA, the inversion of impedance matrix of the inside object is required. This procedure is very time-consuming if the dimension of impedance matrix is very large (like 100000×100000). So one equivalence surface should not enclose many array elements. In this paper, each equivalence surface encloses only one element.

5. NUMERICAL RESULTS

In this section, several numerical results are given to demonstrate the accuracy and efficiency of the proposed method. Firstly, two PEC spheres are computed in free space to analysis the accuracy of the EPA and T-EPA methods. Two spheres are identical with a radius of 0.4 m. The distance between the centers of two spheres is 2 m. Each sphere is enclosed by a cube with a length of 1 m. The excitation is $\hat{x}$ polarized plane wave propagating into the negative $\hat{z}$ direction at 0.3 GHz. The bistatic RCS for the HH polarization is shown in Figure 2. The root

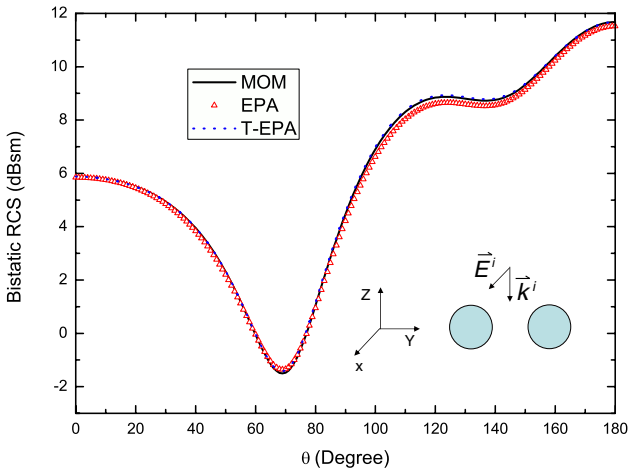

Figure 2. The bistatic RCS of two PEC spheres, HH polarization at 0.3 GHz.

mean square (RMS) error of EPA is 0.1697 dBsm, while the RMS error of T-EPA is 0.0543 dBsm. It is clear that T-EPA is more accurate than EPA.

Secondly, the scattering of 5×5 U-shaped slot micro-strip periodic array antennas is considered. The dimension of the antenna element is shown in Figure 3(a). The PEC strip is coloured with yellow, while the dielectric substrate is coloured with blue. The substrate's thickness is 1.5 cm with $\epsilon_r = 2.2$ and $\mu_r = 1.0$. The dimension of 5×5 array is shown in Figure 3(b). Each element is enclosed by an equivalence surface with the same size of 29 cm $\times$ 21 cm $\times$ 7.5 cm. The volume-surface integral equation (VSIE) [34, 35] is used to solve the scattering currents of the elements. Due to the symmetry of the array, only one **S** matrix needs to be calculated and stored. Therefore, the memory requirement of the array can be reduced. The excitation is $\hat{x}$ polarized plane wave propagating into the negative $\hat{z}$ direction at 2.0 GHz. The bistatic RCS for the HH polarization is shown in Figure 4. A good agreement with the result obtained by traditional VSIE-MLFMA is achieved. Figure 5(a) shows comparison of the number of generalized minimal residual (GMRES) iterations for the 5×5 U-shaped slot micro-strip periodic array antennas between T-EPA with MLFMA and VSIE-MLFMA. It can be seen that the T-EPA hybrid with MLFMA converges to 0.001 with only 15 steps, while the traditional VSIE-MLFMA without preconditioning needs 264 steps. It means that the proposed method can improve the conditioning of the matrix efficiently. The total number of unknowns of the array elements is 3476×25. It is almost the same as the number of unknowns of equivalence surfaces, which is 3552×25. The number of unknowns is

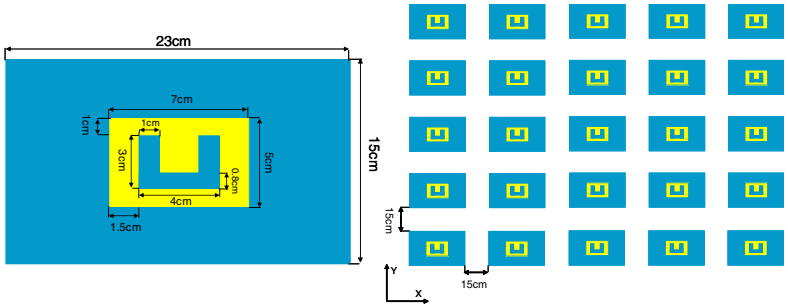

Figure 3. (a) The geometry of a U-shaped slot micro-strip antenna element. (b) The geometry of 5×5 U-shaped slot micro-strip antenna array.

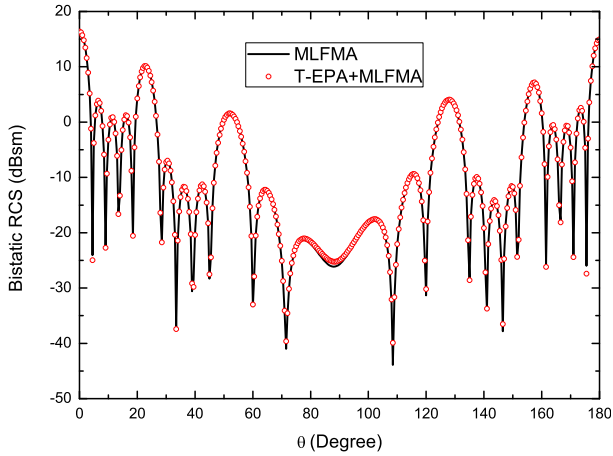

Figure 4. The bistatic RCS of 5×5 U-shaped slot antenna array, HH polarization at 2.0 GHz. Its relative permittivity is $\epsilon_r = 2.2$, relative permeability is $\mu_r = 1.0$.

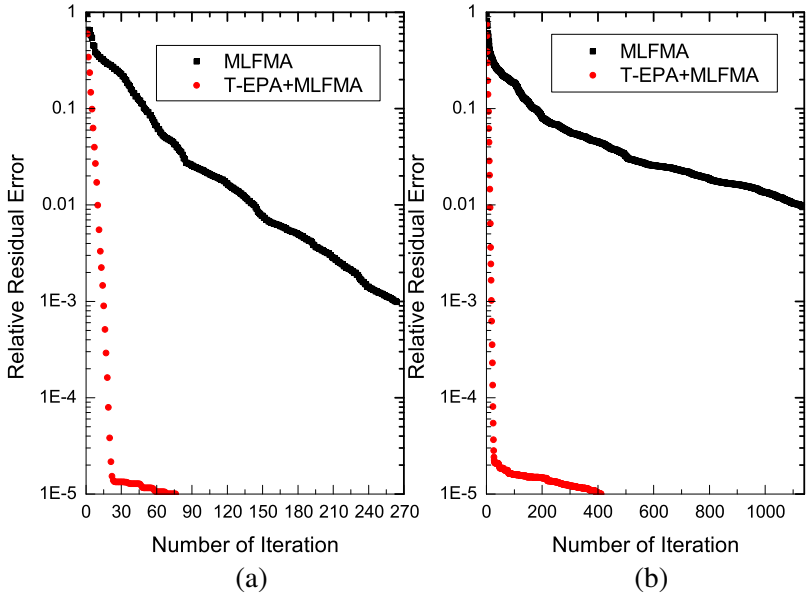

Figure 5. The number of GMRES iterations for the 5×5 U-shaped slot micro-strip periodic array antennas. (a) Each element with relative permittivity $\epsilon_r = 2.2$, relative permeability $\mu_r = 1.0$. (b) Each element with relative permittivity $\epsilon_r = 4.0$, relative permeability $\mu_r = 1.0$.

not reduced in T-EPA method. However, for the element with higher permittivity, the reduction will be significantly. The next example is used to demonstrated that.

In the third example, the element with $\epsilon_r = 4.0$ and $\mu_r = 1.0$ is investigated. The array still consist of 5×5 elements. The other parameters are the same as the second example. The iteration number of GMRES for the array is given in Figure 5(b). For the element with high permittivity, the VSIE-MLFMA needs 1125 steps to converge to 0.01. The T-EPA with MLFMA converges to 0.01 and 0.001 needs 13 steps and 19 steps respectively, which is a bit more than the number of iterations in the second example. The evaluated results of bistatic RCS are plotted in Figure 6. The number of unknowns of equivalence surfaces is still 3552×25, while the total number of unknowns of array elements is changed to 6705×25. The reduction of number of unknowns is 47%. It is obvious that the T-EPA method can reduce the number of unknowns for the objects with high permittivity. The total memory requirement and CPU time for the T-EPA is 605.4 MB and 25679.4 s respectively. In contrast, for traditional MLFMA, the memory requirement is 3204.3 MB, and the CPU time is 46945.0 s.

Fourthly, a non-periodic array is investigated, which is shown in Figure 7. The element is the same as the one in second example, while the distance between two elements is different. The array is illuminated by a plane wave with incidence angle of $\theta^i = 0°$, $\phi^i = 0°$

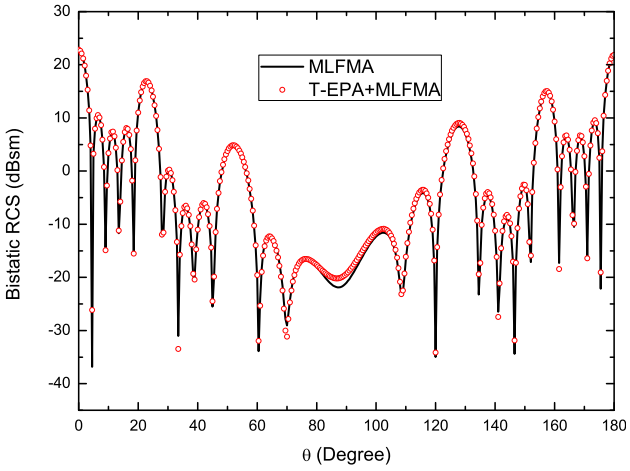

Figure 6. The bistatic RCS of 5×5 U-shaped slot antenna array, HH polarization at 2.0 GHz. Its relative permittivity is $\epsilon_r = 4.0$, relative permeability is $\mu_r = 1.0$.

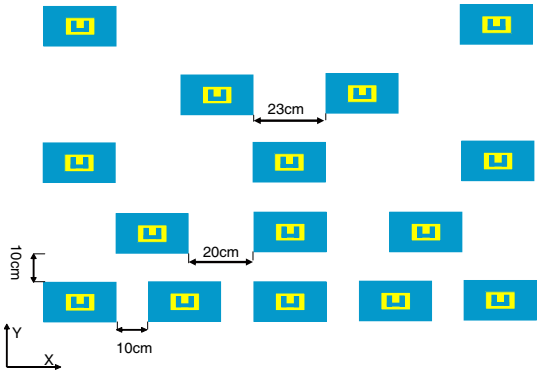

Figure 7. The geometry of non-periodic array with 15 elements. Its relative permittivity is $\epsilon_r = 4.0$, relative permeability is $\mu_r = 1.0$.

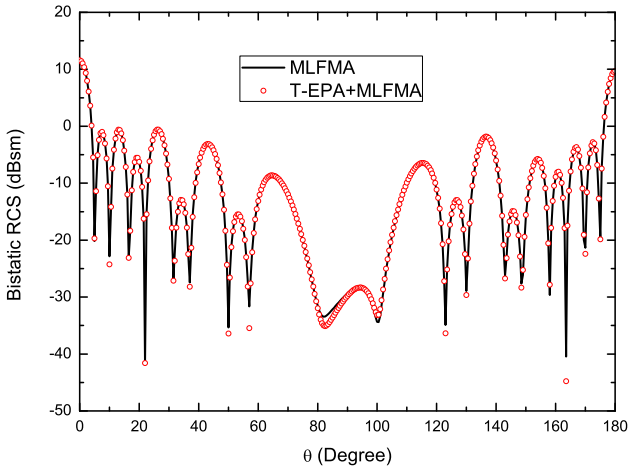

Figure 8. The bistatic RCS of non-periodic array with 15 elements, HH polarization at 2.0 GHz. Its relative permittivity is $\epsilon_r = 4.0$, relative permeability is $\mu_r = 1.0$.

at 2.0 GHz. The results of bistatic RCS for the HH polarization are shown in Figure 8. The results show the well agreement between two methods.

Above four examples have already demonstrated the accuracy and efficiency of the T-EPA hybrid with MLFMA algorithm, next step is to investigate its capability. Finally, to demonstrate the capability of the proposed method for solving large array problems, a periodic array with 40×40 elements are considered. The parameters of the array

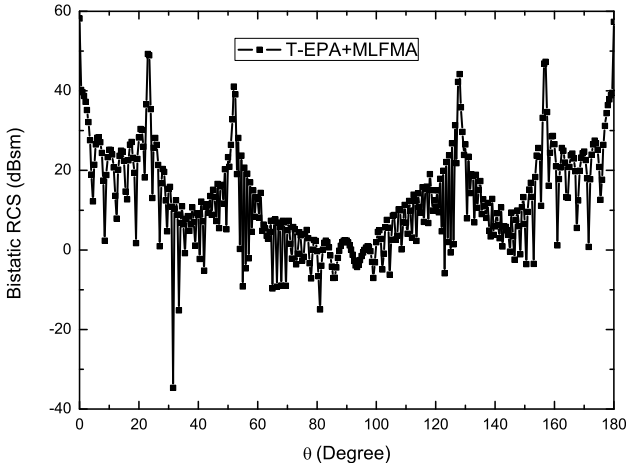

Figure 9. The bistatic RCS of 40×40 U-shaped slot antenna array, HH polarization at 2.0 GHz. Its relative permittivity is $\epsilon_r = 4.0$, relative permeability is $\mu_r = 1.0$.

element is the same as the one in third example, except the number of elements. The total number of unknowns of array elements is 10.728 million (6705×1600). Due to our limited memory, this array can not be solved by traditional VSIE-MLFMA, which needs about 200 GB total memory. By using the T-EPA with MLFMA method, the number of unknowns on the equivalence surfaces is only 5.68 million (3552×1600). The simulation uses 9-levels MLFMA and 26.6 GB total memory. The error converges to 0.001 after 118 iterations. The results of bistatic RCS for the HH polarization are shown in Figure 9. The significant reduction in the memory requirement is mainly based on the following facts: (1) The number of unknowns of the equivalence surfaces is only half of the number of unknowns of the elements. (2) The meshes on the elements are much finer than the meshes on the equivalence surfaces due to the high permittivity. Then finest boxes contain more basis functions in MLFMA. It needs more memory requirement for the computation of nearby regions, which is implemented by MoM. (3) In the T-EPA with MLFMA, the symmetry in radiation and receiving patterns is used as in the surface integral equation case. However, the symmetry does not exist in the VSIE-MLFMA. All of the patterns need to be stored.

6. CONCLUSION

In this paper, the T-EPA combined with MLFMA is used to solve the scattering problems of periodic array and non-periodic array. In this method, each array element is enclosed by a virtual equivalence surface. Each equivalence surface is described by a associated scattering matrix. For the array with the same elements, only one scattering matrix needs to be calculated and stored. By transferring the unknowns of the objects onto the equivalence surfaces, the total number of unknowns can be reduced. The conditioning of the impedance matrix also can be improved. To improve the accuracy of the original EPA, T-EPA is applied. The interaction among equivalence surfaces in T-EPA is further speeded up by MLFMA. The accuracy and efficiency of T-EPA with MLFMA are verified by several results. Especially, the array with 10 million unknowns is solved by this method successfully. As a fast solver for array structures, the present method can realize efficient solution of scattering from periodic array and non-periodic array with complex elements.

ACKNOWLEDGMENT

Thanks to "Natural Science Foundation" (No. 60971032) and the Programme of Introducing Talents of Discipline to Universities under Grant b07046, research funding under G02010201PJ09DZ0212.

REFERENCES

1. Losada, V., R. R. Boix, and F. Medina, "Radar cross section of stacked circular microstrip patches on anisotropic and chiral substrates," *IEEE Trans. Antenn. Propag.*, Vol. 51, No. 5, 1136–1139, May 2003.
2. Gustafsson, M., "RCS reduction of integrated antenna arrays with resistive sheets," *Journal of Electromagnetic Waves and Applications*, Vol. 20, No. 1, 27–40, 2006.
3. Yeo, J. and D. Kim, "Novel tapered AMC structures for backscattered RCS reduction," *Journal of Electromagnetic Waves and Applications*, Vol. 23, No. 5–6, 697–709, 2009.
4. Wang, W. T., S. X. Gong, X. Wang, H. W. Yuan, J. Ling, and T. T. Wan, "RCS reduction of array antenna by using bandstop FSS reflector," *Journal of Electromagnetic Waves and Applications*, Vol. 23, No. 11–12, 1505–1514, 1995.
5. Pozar, D. M. and D. H. Schaubert, "Analysis of an infinite array of

rectangular micristrip patches with idealized feed," *IEEE Trans. Antenn. Propag.*, Vol. 35, No. 10, 1101–1101, Oct. 1984.

6. Liu, Z. F., P. S. Kooi, L. W. Li, M. S. Leong, and T. S. Yeo, "A method of moments analysis of a microtrip phased array in three layered structures," *Progress In Electromagnetics Research*, Vol. 31, 155–179, 2001.
7. Mcgrath, D. T. and V. P. Pyati, "Phased array antenna analysis with the hybrid finite element method," *IEEE Trans. Antennas Propag.*, Vol. 42, No. 12, 1625–1630, Dec. 1994.
8. Hua, Y. and J. Li, "Analysis of longitudinal shunt waveguide slots using FEBI," *Journal of Electromagnetic Waves and Applications*, Vol. 23, No. 14–15, 2041–2046, 2009.
9. Ozgun, O. and M. Kuzuoglu, "Finite element analysis of electromagnetic scattering problems via iterative leap-field domain decomposition method," *Journal of Electromagnetic Waves and Applications*, Vol. 22, No. 2–3, 251–266, 2008.
10. Lee, S. C., M. N. Vouvakis, and J. F. Lee, "A non-overlapping domain decomposition method with non-matching grids for modeling large finite antenna arrays," *J. Comput. Phys.*, Vol. 203, 1–21, Feb. 2005.
11. Holloway, C. L., P. M. McKenna, R. A. Dalke, R. A. Perala, and C. L. Devor, "Time-domain modeling, characterization, and measurements of anechoic and semi-anechoic electromagnetic test chambers," *IEEE Trans. Electro. Compat.*, Vol. 44, No. 1, 102–118, Feb. 2002.
12. Song, J. M., C. C. Lu, and W. C. Chew, "Multilevel fast multipole algorithm for electromagnetic scattering by large complex objects," *IEEE Trans. Antenn. Propag.*, Vol. 45, 1488–1493, Oct. 1997.
13. Hu, J. and Z. P. Nie, "Multilevel fast multipole algorithm for solving scattering from 3-D electrically large object," *Chinese Journal of Radio Science*, Vol. 19, 509–514, May 2004.
14. Wallen, H. and J. Sarvas, "Translation procedures for broadband MLFMA," *Progress In Electromagnetics Research*, Vol. 55, 47–78, 2005.
15. Ouyang, J., F. Yang, S. W. Yang, and Z. P. Nie, "Exact simulation method VSWIE+MLFMA for analysis radiation pattern of pro-feed conformal microstrip antennas and the application of synthesis radiation pattern of conformal array mounted on finite-length PEC circular cylinder with des," *Journal of Electromagnetic Waves and Applications*, Vol. 21, No. 14, 1995–2008, 2007.

16. Hu, J., Z. P. Nie, L. Lei, and L. J. Tian, "Fast solution of scattering from conducting structures by local MLFMA based on improved electric field integral equation," *IEEE Trans. Electromagn. Compat.*, Vol. 50, No. 4, Nov. 2008.
17. Ping, X. W., T. J. Cui, and W. B. Lu, "The combination of bcgstab with multifrontal algorithm to solve FEBI-MLFMA linear systems arising from inhomogeneous electromagnetic scattering problems," *Progress In Electromagnetics Research*, Vol. 93, 91–105, 2009.
18. Peng, Z., X. Q. Sheng, and F. Yin, "An efficient twofold iterative algorithm of FE-BI-MLFMA using multilevel inverse-based ilu preconditioning," *Progress In Electromagnetics Research*, Vol. 93, 369–384, 2009.
19. Taboada, J. M., M. G. Araujo, J. M. Bertolo, L. Landesa, F. Obelleiro, and J. L. Rodriguez, "MLFMA-FFT parallel algorithm for the solution of large-scale problems in elemtromagnetic," *Progress In Electromagnetics Research*, Vol. 105, 15–30, 2010.
20. Blesznski, E. and M. Bleszynski, "AIM: Adaptive integral method for solving large scale electromagnetic scattering and radiation problems," *Radio Science*, Vol. 31, 1225–1251, Sep. 1996.
21. Hu, L., L. W. Li, and T. S. Yeo, "Analysis of scattering by large inhomogeneous bi-anisotropic objects using AIM," *Progress In Electromagnetics Research*, Vol. 99, 21–36, 2009.
22. Seo, S. M. and J.-F. Lee, "A fast IE-FFT algorithm for solving PEC scattering problems," *IEEE Transactions on Magnetics*, Vol. 41, No. 9, 1476–1479, Oct. 1997.
23. Yin, J. L., J. Hu, X. F. Que, and Z. P. Nie, "A fast IE-FFT solution of 3D coating scatterers," *Micro. Opt. Tech. Lett.*, Vol. 52, No. 1, 241–244, Jan. 2010.
24. Li, M. K. and W. C. Chew, "A domain decomposition scheme based on equivalence theorem," *Micro. Opt. Tech. Lett.*, Vol. 48, No. 9, 1853–1857, Sep. 2006.
25. Li, M. K. and W. C. Chew, "Using tap basis to implement the equivalence principle algorithm for domain decomposition in integral equations," *Micro. Opt. Tech. Lett.*, Vol. 48, No. 11, 2218–2222, Nov. 2006.
26. Li, M. K. and W. C. Chew, "Wave-field interaction with complex structures using equivalence principle algorithm," *IEEE Trans. Antenn. Propag.*, Vol. 55, No. 1, 130–138, Jan. 2007.
27. Li, M. K. and W. C. Chew, "Multiscale simulation of complex structures using equivalence principle algorithm with high-order

field point sampling scheme," *IEEE Trans. Antenn. Propag.*, Vol. 56, No. 8, 2389–2397, Aug. 2008.

28. Xiao, G. B., J. F. Mao, and B. Yuan, "Generalized transition matrix for arbitrarily shaped scatterers or scatterer groups," *IEEE Trans. Antenn. Propag.*, Vol. 56, No. 12, 3723–3732, Dec. 2008.
29. Yla-Oijala, P. and M. Taskinen, "Electromagnetic scattering by large and complex structures with surface equivalence principle algorithm," *Waves in Random and Complex Media*, Vol. 19, No. 1, Feb. 2009.
30. Yla-Oijala, P. and M. Taskinen, "Solving electromagnetic scattering by multiple targets with surface equivalence principle algorithm," *3rd European Conference on Antenna and Propagation*, 88–92. Mar. 2009.
31. Yla-Oijala, P., O. Ergul, L. Gurel, and M. Taskinen, "Efficient surface integral equation methods for the analysis of complex metamaterial structures," *3rd European Conference on Antenna and Propagation*, 1560–1564, Mar. 2009.
32. Graglia, R. D., D. R. Wilton, and A. F. Peterson, "Higher order interpolatory vector bases for computational electromagnetics," *IEEE Trans. Antenn. Propag.*, Vol. 45, No. 3, 329–342, Mar. 1997.
33. Hu, J., Z. P. Nie, and L. Lin, "Solving 3-D electromagnetic scattering from conducting object by MLFMA with curvilinear RWG basis," *IEEE Antennas and Propagation Society Int. Symp.*, 460–463, 2003.
34. Lu, C. C. and W. C. Chew, "A coupled surface-volume integral equation approach for the calculation of electromagnetic scattering from composite metallic and material targets," *IEEE Trans. Antenn. Propag.*, Vol. 48, No. 12, 1866–1868, Dec. 2000.
35. Yuan, N., T. S. Yeo, X. C. Nie, and L. W. Li, "RCS computation of composite conductiong-dielectric objects with junctions using the hybrid volume-surface integral equation," *Journal of Electromagnetic Waves and Applications*, Vol. 19, No. 1, 19–36, 2005.
36. Velamparambil, S., W. C. Chew, and J. M. Song, "10 Million unknowns: Is it that big?" *IEEE Trans. Antenn. Propag.*, Vol. 45, No. 2, 43–58, Apr. 1997.